JCTC Journal of Chemical Theory and Computation

Article

pubs.acs.org/JCTC

PERI−CC2: A Polarizable Embedded RI-CC2 Method

Tobias Schwabe,*[,†] Kristian Sneskov,[‡,§] Jógvan Magnus Haugaard Olsen,[∥] Jacob Kongsted,[∥] Ove Christiansen,[‡,§] and Christof Hättig[⊥]

[†]Center for Bioinformatics and Institute of Physical Chemistry, University of Hamburg, Bundesstraße 43, D-20146 Hamburg, Germany

[‡]Center for Oxygen Microscopy and Imaging, Department of Chemistry, Aarhus University, Langelandsgade 140, DK-8000 Aarhus C, Denmark

[§]The Lundbeck Foundation Center for Theoretical Chemistry, Department of Chemistry, Aarhus University, Langelandsgade 140, DK-8000 Aarhus C, Denmark

[∥]Department of Physics, Chemistry and Pharmacy, University of Southern Denmark, Campusvej 55, DK-5230 Odense M, Denmark

[⊥]Lehrstuhl für Theoretische Chemie, Ruhr-Universität Bochum, 44801 Bochum, Germany

ABSTRACT: We present a combination of the polarizable embedding (PE) method with the resolution-of-the-identity implementation of the approximate coupled-cluster singles and doubles method CC2. The new approach, termed PERI−CC2, allows one to study excited state phenomena of large solvated molecular systems with an accurate correlated wave function method. Central to the PE approach is the advanced description of the environmental electrostatic potential and inclusion of polarization, and the quintessence of RI-CC2 is efficient access to excited state properties while retaining the accuracy associated with CC theory. To maintain efficiency, an approximate truncated CC2 density is introduced to calculate the PE contributions. Explicitly, we derive the central equations and outline an implementation of polarizable embedding for the RI-CC2 approach. The new method is tested against previous PE−CC2 and PE−CCSD results for solvatochromic shifts, demonstrating how the important effects of polarization are incorporated well with PERI−CC2 but with a dramatically reduced overall computational cost. A follow-up investigation of the solvatochromic shift of uracil in aqueous solution further illustrates the potential of PERI−CC2. We discuss the need to explicitly incorporate several water molecules into the region treated by quantum mechanics in order to obtain a reliable and accurate description of the physical effects when specific solute/solvent interactions as, e.g., hydrogen-bonds are involved.

1. INTRODUCTION

Despite ongoing development of more efficient electronic structure methods, the system size treatable by modern approaches remains limited, a challenge that only increases when general molecular properties in the condensed phase or in biomolecular systems are investigated. The demand for high accuracy calls for the application of post-Hartree−Fock methods with their inherent larger computational cost. Recent efficiency improvements for post-Hartree−Fock methods follow different approaches to decrease the system size limitation: For instance, the computational cost of some methods can be lowered by resolution-of-the-identity techniques (also called density fitting), which enable a faster evaluation of some electron repulsion integrals in the molecular orbital basis.[1−3] The key example of relevance here is the RI-CC2 approach, derived from the approximate coupled-cluster (CC) with singles and doubles method (CC2),[4] which has proven to be a reasonably accurate way to study electronic excited states also for large systems.[5−8] The computational time can similarly be reduced by Cholesky decomposition techniques.[9,10] Another idea is to exploit the relatively short-ranged nature of correlation effects by working in a basis of local orbitals.[11−18] The fragment molecular orbital[19] and the incremental schemes[20−22] also go along this line. Such methods reduce the complexity of the problem by breaking it down into smaller independent tasks. Further, explicitly correlated so-called R12 or F12 methods can be applied to reduce the one-electron basis set requirements.[23−27] Other approaches make use of a reduced virtual orbital space to decrease the cost in the correlation treatment.[28] Of course, combinations of two or more approaches are possible. However, common to all of these methods is that they attempt to treat the full system on an equal footing.

While all of these are promising approaches, they still cannot be applied to systems with several thousand (or more) atoms routinely. For this, an alternative approach is the hybrid quantum mechanical and molecular mechanical method (QM/MM).[29−31] Here, the system is divided into two subsystems. The smaller one contains the region of primary chemical interest and is treated at a quantum mechanical level, while the larger one describes the environment which is assumed to be representable by a classical treatment.

Not only the QM methods themselves have seen some improvements in this context but also the description of the MM region and the interface.[32−41] This is important since an improved accuracy of only one component is not necessarily sufficient for a general quality increase in property descriptions. This fact has been demonstrated for the treatment of environmental effects on electronic excitations with the

Received: May 11, 2012
Published: July 25, 2012

polarizable embedding method (PE).[42] It has been found that a balanced description of mutual polarization effects between the QM and MM region is needed for accurate results. Within the PE method, the MM electrostatic potential is presently described by a multipole expansion of up to octupoles and by induced dipoles, which are obtained in a self-consistent coupling to the QM region. PE has been formulated for DFT[37] as well as for CC,[40] covering in particular CCS, CC2, CCSD, and CCSDR(3).[43] The PE approach is a successor of a previous formulation of QM/MM approaches[44−46] with polarizable force fields. Besides ground-state energies, linear and higher response properties including electronic excitation properties can also be obtained with PE.[47]

In addition to the above cited work, the integration of post-Hartree−Fock methods into QM/MM frameworks has attracted significant interest recently.[48] The PE approach is comparable to the effective fragment potential (EFP) approach,[34,35] which has been combined with EOM-CCSD[49] and CIS(D).[50] The main differences are, on the one hand, that EFP contains energy terms to model nonclassical effects like Pauli repulsion (which are not included in the current formulation of PE) and that, on the other hand, in the EFP method induced dipoles are only obtained approximately while PE includes a self-consistent treatment also in response calculations. Conceptually, PE is also related to the discrete interaction model/QM approach which has been developed to describe nanoparticles classically based on (frequency dependent) induced dipole moments and atom-wise capacitance.[38,39] Further, there is also some correspondence to implicit solvent models which have been combined with higher correlation methods.[51−57] These very efficient approaches to solvent effects can be quite successful, but they are also known to miss important effects of specific solvent interactions. Because of this, accurate but fast QM/MM methods are still an active field of research.

The PE method has been applied successfully in several studies in the context of solvatochromism effects[37,43,47,58−60] and other properties in solution[47,61−63] as well as to study biomolecular systems.[64] Only in some of the studies was PE−CC utilized because its application is still challenging due to the steep scaling of standard CC methods and the fact that there are still limitations to how small the QM part of a system can be for an accurate description. So far, the PE−CC method has not been combined with any of the aforementioned approaches to reduce computational costs in electronic structure theory. In this paper, we present the combination of the PE method with the RI-CC2 approach,[5] yielding a PERI−CC2 method. To maintain efficiency for the new method, a further approximation to the PE−CC method has to be introduced which is based on the use of a truncated CC2 density for the PE contributions. Compared to standard PE−CC2, the effects on excitation energies are shown to be negligible, and the new method is computationally much faster than standard PE−CC2. The PERI−CC2 method is applicable on systems from biomolecular photoactive proteins with large QM regions to solvation effect studies, which typically requires the computation of 100 or more independent configurations of the solute/solvent system.

The outline of the paper is as follows: In section 2, we present the theory for the combination of PE with RI-CC2, and in section 3, we describe briefly how PERI−CC2 has been implemented in the RI-CC2 program of the TURBOMOLE program package such that the low computational costs and storage demands of RI-CC2 are retained. Section 4 contains the specification of computational details underlying the results in section 5, in which we validate the approach by numerical comparison between previously published PE−CCSD benchmark results before we investigate the aqueous shift of the lowest-lying excitation for uracil. Finally, in section 6, we present our conclusions and perspectives.

2. THEORY

The concept and general theory of the PE method for CC as a special approach to QM/MM computations have been detailed before for both ground state optimizations as well as response theory methods.[40] For completeness, we briefly repeat some of the main ideas and equations of PE−CC theory in order to set the stage for the PERI−CC2 approach. Central to the method is the general Lagrangian

$$L_{\mathrm{PE-CC}}(\mathbf{t}, \bar{\mathbf{t}}) = \langle \Lambda | \hat{H}^{\mathrm{QM}} | \mathrm{CC} \rangle + \langle \Lambda | \hat{G}^{\mathrm{es}} | \mathrm{CC} \rangle - \frac{1}{2} \sum_{uv} F_u^{\mathrm{sta}}(\mathbf{D}^{\mathrm{CC}}) R_{uv} F_v^{\mathrm{sta}}(\mathbf{D}^{\mathrm{CC}}) + E^{\mathrm{non-elec}} \tag{1}$$

Here, $\hat{H}^{\mathrm{QM}}$ represents the vacuum electronic Hamiltonian, $\hat{G}^{\mathrm{es}}$ is the electron operator for the interaction with the multipole moments in the MM region, F_u^{sta} an electric field at an MM site u, $\mathbf{D}^{\mathrm{CC}}$ is the unrelaxed CC density, and R_{uv} is a classical polarization response matrix. $E^{\mathrm{non\text{-}elec}}$ subsumes all terms not mentioned before and not related to the coordinates of the electrons (MM site/MM site or nuclei/MM-sites interactions etc.). The CC ansatz is given as the usual exponential parametrization of the wave function $|\mathrm{CC}\rangle = \exp(\hat{T})|\mathrm{HF}\rangle$, with the cluster operator

$$\hat{T} = \hat{T}_1 + \hat{T}_2 + \ldots = \sum_{i}^{n} \sum_{\mu_i} t_{\mu_i} \tau_{\mu_i} \tag{2}$$

generating excitations out of the reference Hartree−Fock state. Here, τ_{μ_i} denotes an i-tuple excitation operator, and the corresponding excitation amplitudes are denoted t_{μ_i}. Note that the Lagrangian depends in a nonlinear manner on both the cluster amplitudes $\mathbf{t}$ and multipliers $\bar{\mathbf{t}}$. For clarification and ease of reference, we have compiled an overview of the index conventions used in this work in Table 1.

Table 1. Conventions for the Use of QM Orbital and MM Site Indices in This Work

index labels	referencing
κ,λ	atomic orbitals
i, j	occupied spatial molecular orbitals
a, b	virtual spatial molecular orbitals
p, q	general spatial molecular orbitals
m, n	general MM site
u, v	polarizable MM site
s, s'	general interaction site

The CC expectation values in eq 1 are given with the help of an auxiliary state

$$\langle \Lambda | = (\langle \mathrm{HF} | + \sum_{\mu_j} \sum_{j} \bar{t}_{\mu_j} \langle \mu_j |) \exp(-\hat{T}) \tag{3}$$

dx.doi.org/10.1021/ct3003749 | J. Chem. Theory Comput. 2012, 8, 3274−3283

The sum runs over all excitations included in the cluster operation in eq 2. With the help of the auxiliary state, the unrelaxed CC density matrix is defiened

$$D_{pq}^{\mathrm{CC}} = \langle \Lambda | \hat{E}_{pq} | \mathrm{CC} \rangle \tag{4}$$

Here, $\hat{E}_{pq}$ are the spin-free one-particle operators in second quantization acting on general spatial molecular orbitals ϕ_p and ϕ_q. Requiring the Lagrangian to be stationary with respect to the CC multipliers and amplitudes leads to the following equations:

$$\frac{\partial L_{\mathrm{PE-CC}}(\mathbf{t}, \bar{\mathbf{t}})}{\partial t_{\nu_j}} = \langle \Lambda | [\hat{H}^{\mathrm{QM}} + \hat{G}(\mathbf{D}^{\mathrm{CC}}), \hat{\tau}_{\nu_j}] | \mathrm{CC} \rangle = 0 \tag{5}$$

$$\frac{\partial L_{\mathrm{PE-CC}}(\mathbf{t}, \bar{\mathbf{t}})}{\partial \bar{t}_{\nu_j}} = \langle \mu_j | \exp(-\hat{T}) \, (\hat{H}^{\mathrm{QM}} + \hat{G}(\mathbf{D}^{\mathrm{CC}})) \exp(\hat{T}) | \mathrm{HF} \rangle = 0 \tag{6}$$

Unlike in the vacuum case, the equations for t_{μ_i} and $\bar{t}_{\mu_i}$ are coupled by the environment coupling operator $\hat{G}(\mathbf{D}^{\mathrm{CC}})$ known from general PE−CC theory

$$\hat{G}(\mathbf{D}^{\mathrm{CC}}) = \hat{G}^{\mathrm{es}} + \hat{G}^{\mathrm{pol}}(\mathbf{D}^{\mathrm{CC}}) \tag{7}$$

with the electrostatic contribution

$$\hat{G}^{\mathrm{es}} = \sum_{m=1}^{M} \sum_{k=0}^{K} \sum_{pq} \Theta_{m,pq}^{(k)} \mathbf{Q}_m^{(k)} \hat{E}_{pq} \tag{8}$$

and the polarization contribution

$$\hat{G}^{\mathrm{pol}}(\mathbf{D}^{\mathrm{CC}}) = \sum_{u=1}^{U} \sum_{pq} \Theta_{u,pq}^{(1)} \mu_u^{\mathrm{ind}}(\mathbf{D}^{\mathrm{CC}}) \hat{E}_{pq} \tag{9}$$

For the derivation of $\hat{G}(\mathbf{D}^{\mathrm{CC}})$, we refer to the corresponding literature.[40] M is the total number of multipole expansion points m, and U is the total number of polarizable sites u, which can but do not have to be equal to M. $\mathbf{Q}_m^{(k)}$ is a multipole moment of kth order located at expansion point m; i.e., for k = 0, it is a point charge, for k = 1, a dipole moment, and so on. Likewise, $\mu_u^{\mathrm{ind}}(\mathbf{D}^{\mathrm{CC}})$ is an induced dipole moment. Finally, general multipole interaction integrals are defined as

$$\Theta_{s',pq}^{(k)} = \frac{(-1)^{k+1}}{k!} \langle \phi_p(\mathbf{r}_i) | \mathbf{T}_{is'}^{(k)} | \phi_q(\mathbf{r}_i) \rangle \tag{10}$$

where the index i refers to an electron and $\mathbf{r}$ to Cartesian coordinates. $\mathbf{T}_{ss'}^{(k)}$ represents interaction tensors defined as

$$\mathbf{T}_{ss'}^{(k)} = \nabla_s^k \frac{1}{(|\mathbf{r}_s - \mathbf{r}'_s|)} \tag{11}$$

where ∇_s^k is a derivative operator of order k with respect to coordinates $\mathbf{r}_s$ of a general interaction site s.

The polarization contribution stems from the induced dipole moments $\mu_u^{\mathrm{ind}}(\mathbf{D}^{\mathrm{CC}})$. Here, the dependence of the induced dipoles on the electron density, and therefore on the electronic wave function, is indicated. They are obtained from

$$\begin{aligned} \mu^{\mathrm{ind}}(\mathbf{D}^{\mathrm{CC}}) &= \mathbf{R}(\mathbf{F}^{\mathrm{nuc}} + \mathbf{F}^{\mathrm{elec}}(\mathbf{D}^{\mathrm{CC}}) + \mathbf{F}^{\mathrm{mul}}) = \mathbf{R}\mathbf{F}^{\mathrm{sta}}(\mathbf{D}^{\mathrm{CC}}) \\ &= \mu^{\mathrm{ind,nuc}} + \mu^{\mathrm{ind,elec}}(\mathbf{D}^{\mathrm{CC}}) + \mu^{\mathrm{ind,mul}} \end{aligned} \tag{12}$$

where $\mathbf{R}$ is a symmetric classical response matrix of dimension $3U \times 3U$ and the static field $\mathbf{F}^{\mathrm{sta}}(\mathbf{D}^{\mathrm{CC}})$ is the sum of the fields due to the nuclei, electrons (depending on the electronic density), and multipoles. The last equality in eq 12 separates the induced moments into contributions derived from the respective field component. $\mathbf{R}$ is defined as

$$\mathbf{R} = \begin{pmatrix} \alpha_1^{-1} & -T_{12}^{(2)} & \cdots & -\mathbf{T}_{1U}^{(2)} \\ -\mathbf{T}_{21}^{(2)} & \alpha_2^{-1} & \ddots & \vdots \\ \vdots & \ddots & \ddots & -\mathbf{T}_{(U-1)U}^{(2)} \\ -\mathbf{T}_{U1}^{(2)} & \cdots & -\mathbf{T}_{U(U-1)}^{(2)} & \alpha_U^{-1} \end{pmatrix}^{-1} \tag{13}$$

The inverse of the polarizability tensors α_u are placed along the diagonal, while the dipole−dipole interaction tensors are found as off-diagonal elements. See earlier PE work for further details and clarification.[37,40]

In order to apply the general concepts of the CC2 approach, the previous equations are reformulated slightly to separate contributions from electron correlation and from the Fock operator $\hat{F}^{\mathrm{PE}}$, obtained from a preceding self-consistent PE−Hartree−Fock calculation. As an aside, note that this also implies that the reference orbitals in PE−CC already incorporate some of the effects of the environment. To achieve this separation, we rewrite the PE−HF energy as

$$E_{\mathrm{PE-HF}} = \langle \mathrm{HF} | \hat{H}^{\mathrm{QM}} + \hat{G}^{\mathrm{es}} | \mathrm{HF} \rangle - \frac{1}{2} \sum_{uv} F_u^{\mathrm{sta}}(\mathbf{D}^{\mathrm{HF}}) R_{uv} F_v^{\mathrm{sta}}(\mathbf{D}^{\mathrm{HF}}) + E^{\mathrm{non\text{-}elec}} \tag{14}$$

We separate the static field into contributions from the PE−HF reference state and those from the correlated wave function by making use of the difference between the SCF density and the fully correlated (unrelaxed) CC density

$$D_{pq}^{\Delta} = D_{pq}^{\mathrm{CC}} - D_{pq}^{\mathrm{HF}} = \langle \Lambda | \hat{E}_{pq} | \mathrm{CC} \rangle - \langle \mathrm{HF} | \hat{E}_{pq} | \mathrm{HF} \rangle \tag{15}$$

Further, it is convenient to introduce the normal ordered operators

$$\hat{O}_N = \hat{O} - \langle \mathrm{HF} | \hat{O} | \mathrm{HF} \rangle \tag{16}$$

which let us reformulate eq 1 to

$$\begin{aligned} L_{\mathrm{PE-CC}}(\mathbf{t}, \bar{\mathbf{t}}) &= E_{\mathrm{PE-HF}} + \langle \Lambda | \hat{H}_N^{\mathrm{QM}} + \hat{G}_N^{\mathrm{es}} | \mathrm{CC} \rangle \\ &\quad - \sum_{uv} \left(F_u^{\mathrm{sta}}(D^{\mathrm{HF}}) + \frac{1}{2} F_u^{\mathrm{elec}}(\mathbf{D}^{\Delta}) \right) \\ &\quad \times R_{uv} F_v^{\mathrm{elec}}(\mathbf{D}^{\Delta}) \end{aligned} \tag{17}$$

$$= E_{\mathrm{PE-HF}} + \langle \Lambda | \hat{F}_N^{\mathrm{PE}} + \hat{W}_N | \mathrm{CC} \rangle - \frac{1}{2} \sum_{uv} F_u^{\mathrm{elec}}(\mathbf{D}^{\Delta}) R_{uv} F_v^{\mathrm{elec}}(\mathbf{D}^{\Delta}) \tag{18}$$

We made use of the definitions

$$\hat{H}_N^{\mathrm{QM}} = \hat{F}_N^{\mathrm{QM}} + \hat{W}_N \tag{19}$$

$$\hat{F}_N^{\mathrm{PE}} = \hat{F}_N^{\mathrm{QM}} + \hat{G}_N(\mathbf{D}^{\mathrm{HF}}) \tag{20}$$

using the same separation of the Hamiltonian into a Fock operator contribution ($\hat{F}_N^{\mathrm{QM}}$) and a fluctuation potential contribution ($\hat{W}_N$) as for the analogue vacuum ansatz and

defining an effective Fock operator consisting of the vacuum part and the PE contributions (including self-consistently obtained induced dipoles at the HF level).

The CC2 model is derived from the CCSD model by approximating the doubles equations to be correct through first order only. In this process, the singles excitations are treated as zeroth order parameters.[4] Consequently, we inspect the PE−CCSD doubles amplitude equation in order to proceed like in the vacuum case. For this aim, it proves rewarding to introduce $\hat{T}_1$-transformed operators $\tilde{O} = \exp(-\hat{T}_1)\,\hat{O}\exp(\hat{T}_1)$ and make a Baker−Campbell−Hausdorff expansion with the PE Fock operator and the fluctuation potential inserted in eq 6 to obtain

$$0 = \langle \mu_2|\tilde{W} + [\hat{F}^{\mathrm{PE}}, \hat{T}_2] + [\tilde{W}, \hat{T}_2] + [\tilde{G}^{\Delta}, \hat{T}_2] + \frac{1}{2}[[\hat{W}, \hat{T}_2], \hat{T}_2]|\mathrm{HF}\rangle \tag{21}$$

We also introduced the environment coupling operator due to correlation effects, which yields

$$\hat{G}^{\Delta}(\mathbf{D}^{\Delta}) = \hat{G}(\mathbf{D}^{\mathrm{CC}}) - \hat{G}(\mathbf{D}^{\mathrm{HF}}) \tag{22}$$

$$= \sum_{u=1}^{U}\sum_{pq}\Theta^{(1)}_{u,pq}\mu_u^{\mathrm{ind,elec}}(\mathbf{D}^{\Delta})\hat{E}_{pq} \tag{23}$$

For brevity, we omit the implicit dependency of $\hat{G}^{\Delta}$ on $\mathbf{D}^{\Delta}$ in the following. Removing terms of higher than first order in eq 21, we are left with

$$0 = \langle \mu_2|\tilde{W} + [\hat{F}^{\mathrm{PE}}, \hat{T}_2] + [\tilde{G}^{\Delta}, \hat{T}_2]|\mathrm{HF}\rangle \tag{24}$$

The first two terms fully match vacuum CC2 theory. We shall comment more on the last term shortly. The singles equations are the same as for PE−CCSD and are thus given by

$$0 = \langle \mu_1|\tilde{G}^{\Delta} + \tilde{W} + [\hat{F}^{\mathrm{PE}}, \hat{T}_1] + [\tilde{G}^{\Delta}, \hat{T}_2] + [\tilde{W}, \hat{T}_2]|\mathrm{HF}\rangle \tag{25}$$

Using canonical PE−HF orbitals, the $\hat{F}^{\mathrm{PE}},\hat{T}_1$ term of the doubles equations simply evaluates to $(\varepsilon_a + \varepsilon_b - \varepsilon_i - \varepsilon_j)t_{ij}^{ab}$ (with ε_i being an orbital energy). However, the $\hat{G}^{\Delta},\hat{T}_2$ term does not simplify in a similar way. Effectively, this prevents an efficient implementation as realized in the RI-CC2 algorithm, which generates the $\mathbf{t}_2$ amplitudes on-the-fly by exploiting the fact that the double-excitation part can be inverted directly. The contribution of $[\tilde{G}^{\Delta},\hat{T}_2]$ would require that the doubles' amplitudes are stored so that the doubles equations can be solved iteratively. This would cause a storage and I/O bottleneck for large systems. Furthermore, it can be argued that $\hat{G}^{\Delta}$ describes a correlation-induced contribution to the embedding potential; thus $[\tilde{G}^{\Delta},\hat{T}_2]$ is not truly a first-order term. This depends upon the reference state, which might or might not already include contributions from a polarizable embedding potential. In the recent formulation of PE−CC, a PE−SCF reference state is applied (in contrast to previous approaches), and thus, the term only introduces higher order effects. However, the inclusion of the doubles amplitudes and Lagrangian multipliers in the density $\mathbf{D}^{\Delta}$ would significantly increase the computational cost and the complexity of the implementation. On the other hand, the correlation contribution to the density should be small in all situations where a second-order single-reference method such as CC2 is applicable. We therefore introduce for the evaluation of the reaction field a CCS-like difference density

$$D_{pq}^{\Delta'} = D_{pq}^{\mathrm{CCS}'} - D_{pq}^{\mathrm{HF}} \tag{26}$$

$$D_{pq}^{\mathrm{CCS}'} = (\langle \mathrm{HF}| + \sum_{\mu_1}\bar{t}^{*}_{\mu_1}\langle \mu_1|)\left(\hat{E}_{pq} + [\hat{E}_{pq}, \hat{T}_1^{*}] + \frac{1}{2}[[\hat{E}_{pq}, \hat{T}_1^{*}], \hat{T}_1^{*}]\right)|\mathrm{HF}\rangle \tag{27}$$

instead of the $\mathbf{D}^{\Delta}$ as derived from the full CC2 density. In eq 27, the asterisk implies that the $\mathbf{t}_1$ amplitudes and $\bar{\mathbf{t}}_1$ multipliers from CC2 are used. Taken together with eq 23, this leads to the approximate coupling operator $\hat{G}^{\Delta'}$. As we shall demonstrate below in the context of response theory, the terms included allow sufficient polarization interaction stemming from the different reaction fields from an excited state compared to the ground state. Ultimately, replacing Δ^{CC2} by Δ' is a major computational simplification allowing the efficiency trademark of RI-CC2 to be fully retained in the PERI−CC2 method. A related simplification has been used in a recent implementation combining the PCM continuum solvation model and CCSD, where the dependency on the multipliers is neglected.[57]

In combination with the previous considerations for the doubles amplitudes, we may define a Lagrangian for the PERI−CC2 model as

$$\begin{aligned} L_{\mathrm{PERI-CC2}}(\mathbf{t}, \bar{\mathbf{t}}) = {} & E_{\mathrm{PE-HF}} + \langle \mathrm{HF}|\hat{W}\left(\hat{T}_1 + \hat{T}_2 + \frac{1}{2}\hat{T}_1^2\right)|\mathrm{HF}\rangle + \sum_{\mu_1}\bar{t}_{\mu_1}\langle \mu_1|\tilde{W} + [\hat{F}^{\mathrm{PE}}, \hat{T}_1] + [\tilde{W}, \hat{T}_2]|\mathrm{HF}\rangle \\ & + \sum_{\mu_2}\bar{t}_{\mu_2}\langle \mu_2|\tilde{W} + [\hat{F}^{\mathrm{PE}}, \hat{T}_2]|\mathrm{HF}\rangle - \frac{1}{2}\sum_{uv}F_u^{\mathrm{elec}}(\mathbf{D}^{\Delta'})R_{uv}F_v^{\mathrm{elec}}(\mathbf{D}^{\Delta'}) \end{aligned} \tag{28}$$

from which all PERI−CC2 equations may be derived.

As above, the stationarity conditions for the Lagrangian determine the PERI−CC2 amplitude equations:

$$\frac{\partial L_{\mathrm{PERI-CC2}}(\mathbf{t}, \bar{\mathbf{t}})}{\partial \bar{t}_{\nu_1}} = \langle \mu_1|\tilde{G}^{\Delta'} + \tilde{W} + [\hat{F}^{\mathrm{PE}}, \hat{T}_1] + [\tilde{W}, \hat{T}_2]|\mathrm{HF}\rangle = 0 \tag{29}$$

$$\frac{\partial L_{\mathrm{PERI-CC2}}(\mathbf{t}, \bar{\mathbf{t}})}{\partial \bar{t}_{\nu_2}} = \langle \mu_2|\tilde{W} + [\hat{F}^{\mathrm{PE}}, \hat{T}_2]|\mathrm{HF}\rangle = 0 \tag{30}$$

and likewise the multiplier equations:

$$\begin{aligned} \frac{\partial L_{\mathrm{PERI-CC2}}(\mathbf{t}, \bar{\mathbf{t}})}{\partial t_{\nu_1}} = {} & \langle \mathrm{HF}|[\tilde{W}, \hat{\tau}_{\nu_1}]|\mathrm{HF}\rangle + \sum_{\mu_1}\bar{t}_{\mu_1}\langle \mu_1|[(\hat{F}^{\mathrm{PE}} + \tilde{W}), \hat{\tau}_{\nu_1}] + [[\tilde{W}, \hat{\tau}_{\nu_1}], \hat{T}_2]|\mathrm{HF}\rangle \\ & + \sum_{\mu_2}\bar{t}_{\mu_2}\langle \mu_2|[\tilde{W}, \hat{\tau}_{\nu_1}]|\mathrm{HF}\rangle + \langle \mathrm{HF}|[\tilde{G}^{\Delta'}, \hat{\tau}_{\nu_1}]|\mathrm{HF}\rangle \\ & + \sum_{\mu_1}\bar{t}_{\mu_1}\langle \mu_1|[\tilde{G}^{\Delta'}, \hat{\tau}_{\nu_1}]|\mathrm{HF}\rangle = 0 \end{aligned} \tag{31}$$

dx.doi.org/10.1021/ct3003749 | J. Chem. Theory Comput. 2012, 8, 3274−3283

$$\frac{\partial L_{\mathrm{PE-CC}}(\mathbf{t},\bar{\mathbf{t}})}{\partial t_{\nu_2}} = \langle \mathrm{HF}|[\hat{W},\hat{\tau}_{\nu_2}]|\mathrm{HF}\rangle + \sum_{\mu_1}\bar{t}_{\mu_1}\langle\mu_1|[\tilde{W},\hat{\tau}_{\nu_2}]|\mathrm{HF}\rangle + \sum_{\mu_2}\bar{t}_{\mu_2}\langle\mu_2|[\hat{F}^{\mathrm{PE}},\hat{\tau}_{\nu_2}]|\mathrm{HF}\rangle = 0 \tag{32}$$

The equations are similar to the vacuum case with the addition of the $\hat{G}^{\Delta'}$ operator. By introducing $\mathbf{D}^{\Delta'}$, the $\hat{G}^{\Delta}$,$\hat{T}_2$ coupling is also effectively removed.

2.1. LINEAR RESPONSE FOR PERI−CC2

A response theory can be developed for PERI−CC2 following previous CC/MM work. While the coupling of amplitude and multipliers in principle causes some additional complexity, we follow the previous strategy of neglecting that complexity in the identification of expressions for transition properties.[44] Accordingly, excitation energies can, as usual within a CC response theory approach, be obtained by solving the eigenvalue problem of the related Jacobian defined as derivative of the cluster equations with respect to the amplitudes:

$$A_{\mu\nu} = \frac{\partial^2 L_{\mathrm{PERI-CC2}}}{\partial\bar{t}_\mu \partial t_\nu} \tag{33}$$

This leads to the following expressions for the four blocks of the PERI−CC2 Jacobian:

$$\text{doubles/doubles: } A_{\mu_2\nu_2} = \delta_{\mu_2\nu_2}(\varepsilon_a + \varepsilon_b - \varepsilon_i - \varepsilon_j) \tag{34}$$

$$\text{doubles/singles: } A_{\mu_2\nu_1} = \langle\mu_2|[\tilde{W},\hat{\tau}_{\nu_1}]|\mathrm{HF}\rangle \tag{35}$$

$$\text{singles/doubles: } A_{\mu_1\nu_2} = \langle\mu_1|[\tilde{W},\hat{\tau}_{\nu_2}]|\mathrm{HF}\rangle \tag{36}$$

$$\text{singles/singles: } A_{\mu_1\nu_1} = \langle\mu_1|[\hat{F}^{\mathrm{PE}} + \tilde{W} + \tilde{G}^{\Delta'},\hat{\tau}_{\nu_1}] + [[\tilde{W},\hat{\tau}_{\nu_1}],\hat{T}_2] + \tilde{G}^{\nu_1}|\mathrm{HF}\rangle \tag{37}$$

Since $\hat{G}^{\Delta'}$ depends through the correlation contribution to the density on the singles amplitudes, one obtains in the singles/singles block $A_{\mu 1\nu 1}$ a contribution from its derivatives with respect to $t_{\nu 1}$:

$$\hat{G}^{\nu_1} = \frac{\partial\hat{G}^{\Delta'}}{\partial t_{\nu_1}} = \sum_{u=1}^{\overline{U}}\sum_{pq}\Theta^{(1)}_{u,pq}\frac{\partial m_u^{\mathrm{ind,elec}}(\mathbf{D}^{\Delta})}{\partial t_{\nu_1}}\hat{E}_{pq} \tag{38}$$

Introducing the operator $\hat{C}_1 = \sum_{v1} c_{v1}\hat{\tau}_{v1}$, the contribution from this operator in a right (singles) transformation with the Jacobian can be evaluated as

$$\sum_{\nu_1}\langle\mu_1|\tilde{G}^{\nu_1}|\mathrm{HF}\rangle c_{\nu_1} = \langle\mu_1|\tilde{G}^{\Delta}(\mathbf{D}^{c_1})|\mathrm{HF}\rangle \tag{39}$$

$$\tilde{G}^{\Delta}(\mathbf{D}^{c_1}) = \sum_{u=1}^{U}\sum_{pq}\Theta^{(1)}_{u,pq}\mu_u^{\mathrm{ind,elec}}(\mathbf{D}^{c_1})\hat{E}_{pq} \tag{40}$$

$$D^{c_1}_{pq} = (\langle\mathrm{HF}| + \sum_{\mu_1}\bar{t}^*_{\mu_1}\langle\mu_1|)\left([\hat{E}_{pq},\hat{C}_1] + \frac{1}{2}[[\hat{E}_{pq},\hat{C}_1],\hat{T}_1]\right)|\mathrm{HF}\rangle = \sum_{\nu_1}\frac{\partial D^{\Delta'}_{pq}}{\partial t_{\nu_1}}c_{\nu_1} \tag{41}$$

Likewise, a left (singles) transformation is given as

$$\sum_{\mu_1}\bar{c}_{\mu_1}\langle\mu_1|\tilde{G}^{\nu_1}|\mathrm{HF}\rangle = (\langle\mathrm{HF}| + \sum_{\mu_1}\bar{t}_{\mu_1}\langle\mu_1|)[\tilde{G}^{\Delta}({}^{\bar{c}_1}D),\tau_{\nu_1}]|\mathrm{HF}\rangle \tag{42}$$

$$\tilde{G}^{\Delta}({}^{\bar{c}_1}\mathbf{D}) = \sum_{u=1}^{U}\sum_{pq}\Theta^{(1)}_{u,pq}\mu_u^{\mathrm{ind,elec}}({}^{\bar{c}_1}\mathbf{D})\hat{E}_{pq} \tag{43}$$

$${}^{\bar{c}_1}D_{pq} = \sum_{\mu_1}\bar{c}_{\mu_1}\langle\mu_1|\hat{E}_{pq} + [\hat{E}_{pq},\hat{T}_1] + \frac{1}{2}[[\hat{E}_{pq},\hat{T}_1],\hat{T}_1]|\mathrm{HF}\rangle = \sum_{\mu_1}\bar{c}_{\mu_1}\frac{\partial D^{\Delta'}_{pq}}{\partial\bar{t}_{\mu_1}} \tag{44}$$

These equations ultimately give the PERI−CC2 eigenvalues and eigenstates of the Jacobian and thus the excitation energies all defined from the Lagrangian in eq 28. Finally, transition moments can also be calculated following completely the implementation described in ref 65.

3. IMPLEMENTATION

To realize the PERI−CC2 model within the RI-CC2 code, the polarizable embedding was also implemented for SCF energies. For the electrostatic contribution (G^{es}), the same strategy as for a point charge embedding can be followed. The multipole interaction integrals are evaluated at the beginning of the SCF procedure and are added to the one-electron part of the Fock operator.

Since the contribution from induced dipoles depends on the electron density, G^{pol} has to be updated in each SCF cycle. This is done by evaluating the field at all polarizable MM sites u based on the density. On the basis of the field, the induced dipoles are calculated from eq 12. Then, the contribution of these dipoles is added to the Fock matrix using the same routine as for evaluating the (fixed) permanent dipole contributions.

To account for the coupled equations needed for obtaining the PE−CC amplitudes and multipliers, an outer loop is implemented in which the amplitudes and multipliers are optimized in a successive manner before $\hat{G}^{\Delta'}$ is updated. As has been found before,[45] this is efficiently done by carrying out only a limited number of microiterations in the amplitude and multiplier solver. However, in contrast to the previous CCSD/MM implementation,[45,46] PERI−CC2 has been found to be less sensitive to the choice of microiterations in some preliminary calculations. Therefore, a conservative setting of four steps in each solver is chosen by default. The outer loop is run until $\hat{G}^{\Delta'}$ is constant within a given threshold, and the usual (vacuum) requirements for optimizing the CC vector function are fulfilled. In case this pragmatic procedure should cause

problems, it is certainly possible to develop an equation solver where the two sets of equations are solved simultaneously, but there are so far no indications that this is necessary.

Then, excitation properties are evaluated as in a regular CC2 calculation, adding the contribution of $\hat{G}^{\Delta'}$ and its derivatives where necessary to the result vectors in the linear transformations with the Jacobian when solving for its eigenvectors and for the transition moment Lagrangian multipliers. To construct the operators, a general density-driven strategy can be applied. As can be seen from eqs 23, 39, and 42, they all depend on a given density. Once the density is available, the operators can all be evaluated in identical fashion. Explicitly, we construct densities in the Λ basis and transform them to the AO basis, where the Λ basis is derived from the $\hat{T}_1$-transformed MO integrals

$$\tilde{x}_{pq} = \sum_{\kappa} \sum_{\lambda} \Lambda^{p}_{\kappa p} \Lambda^{h}_{\lambda q} x_{\kappa\lambda} \tag{45}$$

with the occupied and virtual transformation matrices

$$\Lambda^{p} = \mathbf{C}(1 - \mathbf{t}_1^{T}) \tag{46}$$

$$\Lambda^{h} = \mathbf{C}(1 + \mathbf{t}_1) \tag{47}$$

where $\mathbf{C}$ is the AO coefficient matrix and κ and λ label AOs.[66] From these densities, the field and the induced dipoles as well as the interaction integrals are obtained using the same routines as for the SCF implementation. The necessary densities and their different block structures in the Λ basis can be found in Table 2.

Table 2. Contributions to Densities Needed to Build the Effective Operators in PERI−CC2 Given in $\hat{T}_1$-Transformed Form

density	occ/occ	occ/vir	vir/occ	vir/vir
$\mathbf{D}^{\Delta'}$	0	0	$\bar{t}_{ai}$	0
$\mathbf{D}^{c}_1$	$-\sum_a \bar{t}_{aj} c_{ai}$	$2c_{ai}$	0	$\sum_t \bar{t}_{at} c_{bi}$
$\bar{c}_1\mathbf{D}$	0	0	$\bar{c}_{ai}$	0

4. COMPUTATIONAL DETAILS

The implementation described above has been carried out in a development version of TURBOMOLE 6.3.[67] The validity of the PERI−CC2 model has been tested by comparing it to previously published results, mainly obtained with PE−CCSD. If not stated otherwise the following computational details were applied: Properties in solution are computed from several geometry configurations extracted from classical molecular dynamic runs. The computations are carried out in a QM/MM like fashion normally containing (only) the solute in the QM region. This is done with the PE method. Final results are the averages over all individual computations. The number of configurations varies between 30 and 120. As validated in the previous studies, this is sufficient to reach converged results in those cases where we compare to experimental results. No new simulations were carried out. Instead, configurations from previous works have been used. In those studies, solvent and solute molecules have been treated as rigid entities. Configurations were obtained as snapshots from molecular dynamic simulations based on a polarizable force field approach. They were extracted every tenth picosecond, which is sufficient to have uncorrelated structures. For more details, we refer to the individual publications.[42,58,68]

For the PE computations, the solvent molecules were represented by potentials with up to and including quadrupole moments and anisotropic dipole polarizabilities located on each atomic site (labeled M2P2). The potentials are derived from LoProp[69] calculations based on B3LYP[70,71]/a-aug-cc-pVTZ[72,73] as described in ref 58. The a-aug-cc-pVTZ basis set is a recontraction of aug-cc-pVTZ to an ANO-type basis, which is necessary for the LoProp procedure. For the QM part, the aug-cc-pVDZ basis set[72,73] with according auxiliary basis set[74] has been applied.

5. RESULTS

As a first test, the consequences of the approximation introduced in PERI−CC2—namely, the approximate densities used for the reaction field defining the environment coupling operator—are investigated. For this, the solvatochromic shift for the first $\pi-\pi^*$ excitation of *p*-nitro-phenolate (PNP) in aqueous solution is considered. It has been found that the shift is very sensitive to whether a fully self-consistent treatment of the induced dipoles in response calculations is applied or not.[42] Therefore, it is very likely that any deficiency in the reaction field approximation would show up in this case. Of course, the RI approximation in itself introduces potential errors of a somewhat different character. In order to dissect these different effects, we compare in Table 3 excitation energies and oscillator strengths for the two lowest-lying transitions for a single arbitrary PNP configuration in water or in a vacuum calculated in three different ways: Either using the PE−CC2 model as implemented in DALTON[75] with the full reaction field or using the PERI−CC2 approach as described above with the standard and a very large auxiliary basis set.

We observe a good agreement, indicating that the reaction field and RI approximations do not influence the results significantly. Note that without the RI approximation to CC2, these computations of PNP are already quite demanding, and we therefore limit ourselves to explicitly testing one solvent configuration in this fashion. Rather, we compare with a

Table 3. Comparison of PE−CC2 and PERI−CC2 Results for One Configuration of PNP in Water Surroundings (aq) and a Vacuum (vac) Based on 6-31++G and the aug-cc-pVDZ or the aug-cc-pVQZ Auxiliary Basis Set[a]**

		(PE-)CC2		(PE)RI-CC2[b]		(PE)RI-CC2[c]	
env.	no. exc.	ΔE(exc)	δ	ΔE(exc)	δ	ΔE(exc)	δ
vac	1	3.27	0.5903	3.27	0.5900	3.27	0.5902
	2	3.49	0.0000	3.49	0.0000	3.49	0.0000
aq	1	2.75	0.7056	2.78	0.6834	2.78	0.6836
	2	3.75	0.0000	3.74	0.0000	3.74	0.0000

[a]The excitation energies (ΔE(exc)) and the oscillator strengths (δ) are given in eV and au, respectively. [b]With aug-cc-pVDZ auxiliary basis. [c]With aug-cc-pVQZ auxiliary basis.

previous study[42] using PE(M2P2)-CCSD/6-31++G**. In fact, this serves to test both the capability of RI−CC2 to incorporate the most important correlation effects compared to CCSD, as well as the effects of using simpler forms of reaction field densities. The solvent potential and the geometry configurations are taken from the original study. For each method, PE−CCSD and PERI−CC2, three different environment models are considered: Model 0 does not include any induced dipoles at all in the environment; i.e., no ploarization effects are included. In model 1, the induced dipoles are obtained from the preceding PE−SCF calculation; i.e., the polarization reaction field is kept fixed during the CC iterations also serving to decouple the amplitude and multiplier equations. Finally, in model 3, the fully self-consistent induced dipoles are used as described in section 2. Therefore, any approximations to the densities introduced in the PE treatment only apply to model 3. Note that compared to the reference study, we skipped polarization model 2 (which yields only minor additional effects) but kept notations as introduced previously. A more detailed discussion about the different polarization models can be found in ref 42. The results for PE(M2P2)-CCSD/6-31++G** and PE(M2P2)RI-CC2/6-31++G** and their relative deviations are shown in Figure 1.

For models 0 and 1, the (average) excitation energy is 3.15 eV with PERI−CC2, resulting in a shift of −0.12 eV in comparison to the vacuum result. For model 3, the excitation energy changes to 2.88 eV and a shift of −0.39 eV, respectively. The trend for the three models is the same as has been found before with PE−CCSD (and also with PE-DFT): There is no significant difference between the first two polarization models (0 and 1), but including self-consistent dipole moments also in the response calculation changes the results markedly. While the absolute excitation energies are lower with PERI−CC2 than with PE−CCSD, which yields 3.31 eV (model 0 and 1) and 3.06 eV (model 3), the solvatochromic shifts with respect to the vacuum are in very good agreement. With PE−CCSD, the shifts are −0.14 and −0.15 eV (model 0 and 1) and −0.39 eV (model 3). The additional shift due to model 3 relative to model 1 is −0.25 eV for PE−CCSD and −0.27 eV for PERI−CC2. This shows that the additional approximations in PERI−CC2 do not neglect the main contributions for describing the change of the reaction field upon excitation. This is further supported when the individual deviations between the two methods for each configuration are inspected (Figure 1, bottom). The relative difference in the contribution of each model to the total shift, $\Delta\Delta E$(shift), is plotted there. The average relative differences are −0.02 eV for model 0, −0.01 eV for model 1, and 0.02 eV for model 3. There is no significant increase when going from model 1 to model 3. A deficiency in the additional approximations to the PE method could only be seen in this step. This indicates that differences in the solvatochromic shifts are rooted in the electronic structure methods in use (RI-CC2/6-31++G** vs CCSD/6-31++G**) and not in the way the environment contribution is treated.

So far, the presented results concern one solvent only, namely, water. One of the advantages of discrete solvent models, and the PE method in particular, is the possibility to describe any solvent on equal footing. This is in contrast to implicit solvent models which cover specific solute/solvent interactions less accurately, and as a consequence, relative effects between different solvents cannot always be described to a satisfying extent. This has been demonstrated, e.g., for the solvatochromic shift of acetone in several solvents.[58] PE−CCSD has also been applied for this study, and it thus again provides us with an ideal reference test set for estimating the accuracy of the PERI−CC2 method.

In Figure 2, the solvatochromic shifts obtained with PE(M2P2)-CCSD/aug-cc-pVDZ and PE(M2P2)RI-CC2/aug-cc-pVDZ for the $n-\pi^*$ excitation of acetone are shown. The

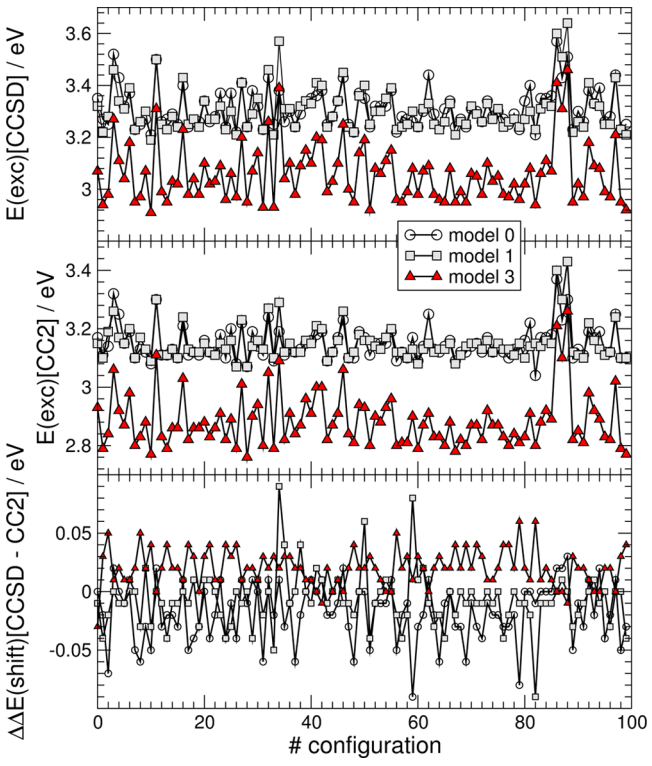

Figure 1. (Top) Electronic excitation energies for the first $\pi-\pi^*$ excitation of PNP in aqueous solution with PE−CCSD/6-31++G** and different models for induced dipole moments (see text). (Middle) Same results with PERI−CC2/6-31++G**. (Bottom) Deviation between PE−CCSD and PERI−CC2 for the effect on the excitation shift introduced by each model.

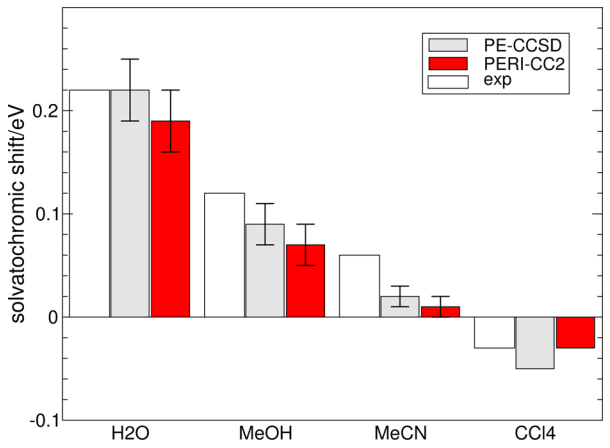

Figure 2. Solvent shift for the $n-\pi^*$ excitation of acetone in different solvents. Both theoretical methods are combined with an M2P2 solvent potential and the aug-cc-pVDZ basis set. Results are obtained from averaging over 30 independent configurations. The standard error of the mean is indicated with bars. Experimental results from ref 76.

dx.doi.org/10.1021/ct3003749 | J. Chem. Theory Comput. 2012, 8, 3274−3283

Table 4. Excitation Energies (ΔE_{sol}) and Solvatochromic Shifts ($\Delta\Delta E_{sol}$) for Uracil in Aqueous Solution Obtained with Different CC2 QM/MM Calculations for the $\pi-\pi^*$ and $n-\pi^*$ Excitations[a]

method	no. QM water	$\Delta E_{sol}^{\pi-\pi*}$	$\Delta\Delta E_{sol}^{\pi-\pi*}$	$\Delta E_{sol}^{n-\pi*}$	$\Delta\Delta E_{sol}^{n-\pi*}$
CC2/MM[b]	0	5.20 ± 0.01	−0.20 ± 0.01	5.37 ± 0.03	0.43 ± 0.03
CC2/MM (best est.)[b,c]	0	5.11 ± 0.01	−0.29 ± 0.01	5.39 ± 0.03	0.45 ± 0.03
PERI−CC2	0	5.16 ± 0.01	−0.24 ± 0.01	5.47 ± 0.03	0.53 ± 0.03
PERI−CC2	4	5.15 ± 0.01	−0.25 ± 0.01	5.37 ± 0.02	0.43 ± 0.02

[a]In all cases, the aug-cc-pVDZ basis set is applied. All energies in eV. [b]Taken from ref 68. [c]Best estimate; corrected for inclusion of 12 QM water and higher order effects (see text).

results are computed for the solvents water, methanol, acetonitrile, and carbon tetrachloride. The configurations and the solvent potentials are taken from previous work.[58] Experimental results,[76] even the small red-shift for CCl_4, are fully recovered by PERI−CC2. The predicted shifts are in excellent agreement with the PE−CCSD results with deviations well below 0.05 eV. The absolute excitation energies are slightly overestimated by both methods, exceeding experimental results by about 0.1 eV. This is a constant shift regardless of the environment—even for vacuum. This, again, underlines the possibility of treating different environments equally well with the PE method.

Having thus established the reliability of the PERI−CC2 approach compared to PE−CCSD, we turn the focus toward the lowest-lying excited states of uracil in aqueous solution. In a previous investigation,[68] it was found that the solvatochromic shift is far from easy to describe by more traditional theoretical means. A straightforward QM/MM approach based on CC2 (without the resolution of identity) including a solvent potential with point charges and isotropical polarizabilities showed qualitative agreement with experimental results. Further tests revealed that this solvent potential was not able to describe all important effects. In principle, this could have been overcome by including water molecules next to the solute into the QM region because the missing effects are most likely very short-ranged and quantum mechanical in nature. However, this was not possible previously because the computational cost exceeded what was affordable. Therefore, the missing contributions due to the insufficient water potential were estimated pragmatically via related test calculations, ultimately yielding an additional shift of 0.09 eV. With PERI−CC2, we may return to this unsettled issue of predicting the accurate shift of uracil in water with systematic CC calculations.

Using the same 120 configurations as before,[68] we repeat the calculations with PERI−CC2/aug-cc-pVDZ and a more sophisticated M2P2 water potential. Because of the efficiency of the method, calculations including four water molecules in the QM region (each of them next to one of the four H-bond acceptors in uracil) can also be carried out. These 120 computations with 384 basis functions each could not have been performed economically without our new implementation. The results along with previous ones are listed in Table 4.

The experimental result[77−80] for the shift of the $\pi-\pi^*$ excitation is −0.30 eV, and PERI−CC2 is thus seen to agree nicely (−0.24 eV). It improves also on the previous CC2/MM result (−0.20 eV). The better performance can primarily be attributed to the improved solvent potential (quadrupoles as compared to charges only). For completeness, note that there are minor conceptual differences in how the polarization coupling to the environment is treated in the two calculations; this is unlikely to influence the outcome. This can also be deduced from the best estimate result from ref 68, where the influence of a higher level treatment of the surroundings is estimated. Somewhat surprisingly, including four water molecules in the QM region has virtually no effect on the PERI−CC2 result. This is quite encouraging that such an improved description can be achieved with a more sophisticated classical potential; previously,[68] it has been speculated that the missing effects are related to solute−solvent dispersion interactions which are not easily modeled across a QM/MM interface. On the basis of the PE(M2P2)RI-CC2/aug-cc-pVDZ results presented here, this seems not to be necessary.

For the $n-\pi^*$ transition, the picture is less clear. The PERI−CC2 excitation energy is 5.47 eV and decreases by 0.10 eV, including water in the QM region, thus showing a larger effect than for the lowest excited state. For both excited states, it should be noted that the effects found are different than in the previous CC2/MM uracil study carried out with a simpler potential. For a complete understanding, the effect of the different water potentials has to be investigated in more detail.

6. CONCLUSION AND SUMMARY

In this paper, the derivation and implementation of a combined QM and MM approach based on the RI-CC2 ansatz and the polarizable embedding method is presented, dubbed PERI−CC2. It enables a very efficient treatment of environment effects on both ground and excited state properties by describing the perturbing environment effects in a classical fashion but retaining the major effects of incorporating fully self-consistent polarization. Thereby, the PE method ensures an increased accuracy by taking induced moments in the MM region into account. To uphold the computational efficiency of RI-CC2, a PERI−CC2 tailored approximation for the polarization treatment is introduced. The results obtained using this approximate reaction field are validated against corresponding PE−CC2 calculations, and very good agreement is observed. Especially, we show that PERI−CC2 is fully capable of incorporating polarization effects even within linear response calculations of excitation energies. Likewise, it shows the same sensitivity to a broad range of solvent potentials by reproducing the most important trends obtained at the PE−CCSD level of theory—with a dramatically reduced computational cost.

Finally, solvatochromic shifts of uracil in aqueous solution have been investigated. PERI−CC2 shows better agreement with experimental results for the $\pi-\pi^*$ excitation than previous computations and is in good agreement with best estimate results. Likewise, the values are converged with respect to the inclusion of solvent molecules into the QM region. For the $n-\pi^*$ excitation, the latter does not hold completely. This might be related to a deficiency in the solvent potential or perhaps in the QM/MM interface treatment. Further investigations in that direction have to be carried out to come to a final conclusion.

Regardless of the individual outcome for the two excitations, the results demonstrate that it is possible to describe even a challenging case like uracil in aqueous solution with the PE method. This requires the inclusion of many different effects: an accurate QM method like CC, the inclusion of polarization effects from the classical surroundings, and a sophisticated electrostatic potential for the environment. Additionally, the PERI−CC2 approach meets the demand for very efficient methods allowing for large QM regions to be used in QM/MM calculations. This is important also as a benchmarking tool in turn verifying the accuracy of lower level methods.

Of course, the application range of PERI−CC2 is not limited to systems in solution. With PERI−CC2, it is now possible to apply CC for biomolecular problems where local phenomena are of interest and an embedding scheme can be used. Likewise, one can think of applications for molecules on surfaces or molecules embedded in a polymer matrix—typical situations for the study of solar cells on the molecular level.

AUTHOR INFORMATION

Corresponding Author

*E-mail: schwabe@zbh.uni-hamburg.de.

Notes

The authors declare no competing financial interest.

ACKNOWLEDGMENTS

T.S. acknowledges support through a Feodor-Lynen fellowship from the Alexander von Humboldt Foundation. O.C. acknowledges support from the Danish Center for Scientific Computing (DCSC), the Danish national research foundation, the Lundbeck Foundation, and EUROHORCs for a EURYI award. J.K. thanks the DCSC, The Danish Councils for Independent Research (STENO and Sapere Aude programmes), the Lundbeck Foundation, and the Villum foundation for financial support.

REFERENCES

(1) Vahtras, O.; Almlöf, J.; Feyereisen, M. *Chem. Phys. Lett.* **1993**, *213*, 514−518.
(2) Feyereisen, M.; Fitzgerald, G.; Komornicki, A. *Chem. Phys. Lett.* **1993**, *208*, 359−363.
(3) Weigend, F.; Häser, M. *Theor. Chem. Acc.* **1997**, *97*, 331−340.
(4) Christiansen, O.; Koch, H.; Jørgensen, P. *Chem. Phys. Lett.* **1995**, *243*, 409−418.
(5) Hättig, C.; Weigend, F. *J. Chem. Phys.* **2000**, *113*, 5154−5161.
(6) Köhn, A.; Hättig, C. *J. Chem. Phys.* **2003**, *119*, 5021−5036.
(7) Send, R.; Kaila, V. R. I.; Sundholm, D. *J. Chem. Theory Comput.* **2011**, *7*, 2473−2484.
(8) Kats, D.; Schütz, M. *J. Chem. Phys.* **2009**, *131*, 124117.
(9) Beebe, N. H. F.; Linderberg, J. *Int. J. Quantum Chem.* **1977**, *12*, 683−705.
(10) Koch, H.; de Merás, A. S.; Pedersen, T. B. *J. Chem. Phys.* **2003**, *118*, 9481−9484.
(11) Pulay, P.; Saebø, S. *Theor. Chim. Acta* **1986**, *69*, 357−368.
(12) Saebø, S.; Pulay, P. *J. Chem. Phys.* **1987**, *86*, 914−922.
(13) Schütz, M.; Hetzer, G.; Werner, H.-J. *J. Chem. Phys.* **1999**, *111*, 5691−5705.
(14) Neese, F.; Wennmohs, F.; Hansen, A. *J. Chem. Phys.* **2009**, *130*, 114108.
(15) Neese, F.; Hansen, A.; Liakos, D. G. *J. Chem. Phys.* **2009**, *131*, 064103.
(16) Freundorfer, K.; Kats, D.; Korona, T.; Schütz, M. *J. Chem. Phys.* **2010**, *133*, 244110.
(17) Ziółkowski, M.; Jansík, B.; Kjærgaard, T.; Jørgensen, P. *J. Chem. Phys.* **2010**, *133*, 014107.
(18) Helmich, B.; Hättig, C. *J. Chem. Phys.* **2011**, *135*, 214106.
(19) Kitaura, K.; Ikeo, E.; Asada, T.; Nakano, T.; Uebayasi, M. *Chem. Phys. Lett.* **1999**, *313*, 701−706.
(20) Stoll, H. *Phys. Rev. B* **1992**, *46*, 6700−6704.
(21) Friedrich, J.; Hanrath, M.; Dolg, M. *Z. Phys. Chem.* **2010**, *224*, 513−525.
(22) Mata, R. A.; Stoll, H. *J. Chem. Phys.* **2011**, *134*, 034122.
(23) Kutzelnigg, W. *Theor. Chem. Acta* **1985**, *68*, 445−469.
(24) Shiozaki, T.; Kamiya, M.; Hirata, S.; Valeev, E. F. *J. Chem. Phys.* **2008**, *129*, 071101.
(25) Köhn, A. *J. Chem. Phys.* **2009**, *130*, 104104.
(26) Hättig, C.; Tew, D. P.; Köhn, A. *J. Chem. Phys.* **2010**, *132*, 231102.
(27) Hättig, C.; Klopper, W.; Köhn, A.; Tew, D. P. *Chem. Rev.* **2012**, *112*, 4−74.
(28) Send, R.; Kaila, V. R. I.; Sundholm, D. *J. Chem. Phys.* **2011**, *134*, 214114.
(29) Warshel, A.; Levitt, M. *J. Mol. Biol.* **1976**, *103*, 227−249.
(30) Lin, H.; Truhlar, D. G. *Theor. Chem. Acc.* **2007**, *117*, 185−199.
(31) Senn, H. M.; Thiel, W. *Angew. Chem., Int. Ed.* **2009**, *48*, 1198−1229.
(32) Thompson, M. A. *J. Chem. Phys.* **1996**, *100*, 14492−14507.
(33) Gao, J.; Byun, K. *Theor. Chem. Acc.* **1997**, *96*, 151−156.
(34) Gordon, M. S.; Freitag, M. A.; Bandyopadhyay, P.; Jensen, J. H.; Kairys, V.; Stevens, W. J. *J. Phys. Chem. A* **2001**, *105*, 293−307.
(35) Gordon, M. S.; Slipchenko, L. V.; Li, H.; Jensen, J. H. *Annu. Rep. Comput. Chem.* **2007**, *3*, 177−193.
(36) Xie, W.; Gao, J. *J. Chem. Theory Comput.* **2007**, *3*, 1890−1900.
(37) Olsen, J. M.; Aidas, K.; Kongsted, J. *J. Chem. Theory Comput.* **2010**, *6*, 3721−3734.
(38) Morton, S. M.; Jensen, L. *J. Chem. Phys.* **2010**, *133*, 074103.
(39) Morton, S. M.; Jensen, L. *J. Chem. Phys.* **2011**, *135*, 134103.
(40) Sneskov, K.; Schwabe, T.; Kongsted, J.; Christiansen, O. *J. Chem. Phys.* **2011**, *134*, 104108.
(41) Kawashima, Y.; Nakano, H.; Jung, J.; Ten-no, S. *Phys. Chem. Chem. Phys.* **2011**, *13*, 11731−11738.
(42) Sneskov, K.; Schwabe, T.; Christiansen, O.; Kongsted, J. *Phys. Chem. Chem. Phys.* **2011**, *13*, 18551−18560.
(43) Sneskov, K.; Matito, E.; Kongsted, J.; Christiansen, O. *J. Chem. Theory Comput.* **2010**, *6*, 839−850.
(44) Kongsted, J.; Osted, A.; Christiansen, O.; Mikkelsen, K. V. *Mol. Phys.* **2002**, *100*, 1813−1828.
(45) Kongsted, J.; Osted, A.; Mikkelsen, K. V.; Christiansen, O. *J. Phys. Chem. A* **2003**, *107*, 2578−2588.
(46) Kongsted, J.; Osted, A.; Mikkelsen, K. V.; Christiansen, O. *J. Chem. Phys.* **2003**, *118*, 1620−1633.
(47) Olsen, J. M. H.; Kongsted, J. In *Advances in Quantum Chemistry*; Sabin, J. R., Brändas, E., Eds.; Academic Press: New York, 2011; Vol. *61*, pp 107−143.
(48) Mata, R. A. *Phys. Chem. Chem. Phys.* **2010**, *12*, 5041−5052.
(49) Slipchenko, L. V. *J. Phys. Chem. A* **2010**, *114*, 8824−8830.
(50) Kosenkov, D.; Slipchenko, L. V. *J. Phys. Chem. A* **2011**, *115*, 392−401.
(51) Christiansen, O.; Mikkelsen, K. V. *J. Chem. Phys.* **1999**, *110*, 1365−1375.
(52) Christiansen, O.; Mikkelsen, K. V. *J. Chem. Phys.* **1999**, *110*, 8348−8360.
(53) Cammi, R. *J. Chem. Phys.* **2009**, *131*, 164104.
(54) Caricato, M.; Mennucci, B.; Scalmani, G.; Trucks, G. W.; Frisch, M. J. *J. Chem. Phys.* **2010**, *132*, 084102.
(55) Caricato, M.; Scalmani, G.; Trucks, G. W.; Frisch, M. J. *J. Phys. Chem. Lett.* **2010**, *1*, 2369−2373.
(56) Cammi, R.; Fukuda, R.; Ehara, M.; Nakatsuji, H. *J. Chem. Phys.* **2010**, *133*, 024104.
(57) Caricato, M. *J. Chem. Phys.* **2011**, *135*, 074113.
(58) Schwabe, T.; Olsen, J. M. H.; Sneskov, K.; Kongsted, J.; Christiansen, O. *J. Chem. Theory Comput.* **2011**, *7*, 2209−2217.
(59) Murugan, N. A.; Kongsted, J.; Rinkevicius, Z.; Ågren, H. *Phys. Chem. Chem. Phys.* **2011**, *13*, 1290−1292.

(60) Murugan, N. A.; Kongsted, J.; Rinkevicius, Z.; Aidas, K.; Mikkelsen, K. V.; Ågren, H. *Phys. Chem. Chem. Phys.* **2011**, *13*, 12506−12516.
(61) Kjaer, H.; Sauer, S. P. A.; Kongsted, J. *J. Chem. Phys.* **2011**, *134*, 044514.
(62) Rinkevicius, Z.; Murugan, N. A.; Kongsted, J.; Aidas, K.; Steindal, A. H.; Ågren, H. *J. Phys. Chem. B* **2011**, *115*, 4350−4358.
(63) Eriksen, J. J.; Olsen, J. M. H.; Aidas, K.; Ågren, H.; Mikkelsen, K. V.; Kongsted, J. *J. Comput. Chem.* **2011**, *32*, 2853−2864.
(64) Rocha-Rinza, T.; Sneskov, K.; Christiansen, O.; Ryde, U.; Kongsted, J. *Phys. Chem. Chem. Phys.* **2011**, *13*, 1585−1589.
(65) Hättig, C.; Köhn, A. *J. Chem. Phys.* **2002**, *117*, 6939−6951.
(66) Koch, H.; Christiansen, O.; Kobayashi, R.; Jørgensen, P.; Helgaker, T. *Chem. Phys. Lett.* **1994**, *228*, 233−238.
(67) *TURBOMOLE*, V6.3 2011; University of Karlsruhe and Forschungszentrum Karlsruhe GmbH: Karlsruhe, Germany, 1989−2007; TURBOMOLE GmbH: Karlsruhe, Germany, 2007. Available from http://www.turbomole.com (accessed August 2012).
(68) Olsen, J. M.; Aidas, K.; Mikkelsen, K. V.; Kongsted, J. *J. Chem. Theory Comput.* **2010**, *6*, 249−256.
(69) Gagliardi, L.; Lindh, R.; Karlström, G. *J. Chem. Phys.* **2004**, *121*, 4494−5000.
(70) Becke, A. D. *J. Chem. Phys.* **1993**, *98*, 5648−5652.
(71) Stephens, P. J.; Devlin, F. J.; Chabalowski, C. F.; Frisch, M. J. *J. Phys. Chem.* **1994**, *98*, 11623−11627.
(72) Dunning, T. H. *J. Chem. Phys.* **1989**, *90*, 1007−1023.
(73) Kendall, R. A.; T. H. Dunning, J.; Harrison, R. J. *J. Chem. Phys.* **1992**, *96*, 6796−6806.
(74) Weigend, F.; Köhn, A.; Hättig, C. *J. Chem. Phys.* **2002**, *116*, 3175−3183.
(75) DALTON2011. http://www.daltonprogram.org (accessed April 1, 2012).
(76) Renge, I. *J. Phys. Chem. A* **2009**, *113*, 10678−10686.
(77) Voet, D.; Gratzer, W. B.; Cox, R. A.; Doty, P. *Biopolymers* **1963**, *1*, 193−208.
(78) B., C. L.; Peschel, G. G.; I., T., Jr. *J. Phys. Chem.* **1965**, *69*, 3615−3618.
(79) Daniels, M.; Hauswirth, W. *Science* **1971**, *171*, 675−677.
(80) Du, H.; Fuh, R.; Li, J.; Corkan, L.; Lindsey, J. *Photochem. Photobiol.* **1998**, *68*, 141−142.